Solid State Sciences 63 (2017) 16–22

Contents lists available at ScienceDirect

Solid State Sciences

journal homepage: www.elsevier.com/locate/ssscie

Synthesis, crystal structure, vibrational spectroscopy and expected magnetic properties of a new bismuth nickel phosphate $Ni(BiO)_2(PO_4)(OH)$ with a namibite-type structure

Sergey M. Aksenov [a, b, *], Vladimir S. Mironov [b], Elena Yu. Borovikova [c], Natalia A. Yamnova [c], Olga A. Gurbanova [c], Anatoly S. Volkov [c], Olga V. Dimitrova [c], Dina V. Deyneko [d]

[a] Institute of Organoelement Compounds RAS, Vavilova Street 28, Moscow, 119334, Russian Federation
[b] Institute of Crystallography of Federal Scientific Research Centre "Crystallography and Photonics", Russian Academy of Sciences, Leninskiy Prospekt 59, Moscow, 119333, Russian Federation
[c] Faculty of Geology, Moscow State University, Vorobievy Gory, Moscow, 119991, Russian Federation
[d] Faculty of Chemistry, Moscow State University, Vorobievy Gory, Moscow, 119991, Russian Federation

ARTICLE INFO

Article history:
Received 8 August 2016
Received in revised form
4 October 2016
Accepted 6 November 2016
Available online 9 November 2016

Keywords:
Hydrothermal synthesis
Bismuth nickel oxophosphate
Namibite
Single-crystal X-ray diffraction
Magnetic properties

ABSTRACT

Single crystals of a novel Bi–Ni phosphate $Ni(BiO)_2(PO_4)(OH)$ were synthesized by a hydrothermal method in Bi_2O_3–NiO–K_2O–P_2O_5 system and characterized by X-ray structure analysis and IR and Raman spectroscopy. This compound crystallizes in a namibite type structure with triclinic unit-cell parameters, $a = 6.3220$ (3) Å, $b = 6.9043$ (4) Å, $c = 7.5641$ (5) Å, $\alpha = 90.483$ (5)°, $\beta = 107.219$ (5)°, $\gamma = 110.758$ (5)°; $V = 292.51$ (3) Å^3; space group $P\bar{1}$ (No. 2). Crystal structure is refined to final $R_1 = 4.09$ using 1637 $I > 2\sigma(I)$. The structure contains infinite chains $\{Ni(OH)(PO_4)\}_\infty$ built of corner-sharing NiO_6 octahedra. Microscopic calculations of the intra- and interchain J (Ni–Ni) exchange parameters suggests possible $S = 1$ antiferromagnet chain behavior of this compound at low temperatures.

1. Introduction

Bismuth oxides and bismuth-based oxo-salts of transition metal ions are well-known classes of inorganic compounds that attract interest due to a wide range of physical and chemical properties, such as luminescence, selective oxidation catalysts, and multiferroic behavior [1–4]. They are characterized by a wide structural diversity associated with edge-sharing OBi_4 tetrahedra forming 0D, 1D, 2D and 3D polycationic frameworks; very often mixed $O(Bi,M)_4$ tetrahedra are formed due to entering transition metal ions [5]. Many of these compounds belong to the Bi_2O_3–MO–X_2O_5 ternary system (M – divalent metals; X = P, As, V) [6–17]. Among them, bismuth-nickel compounds with 1D and 2D structures containing six-coordinated high-spin Ni^{2+} ions are of interest because of their potential low-dimensional magnetic properties. However, currently known bismuth nickel oxo-salts are represented by only few synthetic compounds (BiNiO)(PO_4) [18], $Bi_{6.56}Ni_{0.44}P_2O_{15.2}$ [19], $BiNi_2BPO_2O_{10}$ [20] and natural mineral paganoite (BiNiO)(AsO_4) [21].

In this paper we report hydrothermal synthesis, single crystal X-ray structure analysis and vibrational spectra of a novel bismuth nickel phosphate $Ni(BiO)_2(PO_4)(OH)$ related to mineral namibite and evaluate its potential magnetic properties.

2. Experimental

2.1. Synthesis and characterisation

Single crystals of Bi-Ni phosphate $Ni(BiO)_2(PO_4)(OH)$ were synthesized by a hydrothermal method. Standard Cu-lined stainless steel autoclave of 16 ml capacity was used. The coefficient of the autoclave filling was selected so that pressure was constant. The

* Corresponding author. Institute of Organoelement Compounds RAS, Vavilova Street 28, Moscow, 119334, Russian Federation.
E-mail address: aks.crys@gmail.com (S.M. Aksenov).

http://dx.doi.org/10.1016/j.solidstatesciences.2016.11.003
1293-2558/

synthesis was carried out at the general pressure of 480–500 atm in the temperature range from 690 K to 700 K. The bottom temperature point was limited by kinetics of the chemical reaction while the upper point was limited by equipment characteristics. The experiment duration is 20 days and it corresponds to full completion of the chemical reaction. The following analytical-grade compounds were used: $Bi(OH)_3$, $NiCO_3$, K_2CO_3, K_3PO_4. The synthesis was carried out with the Bi_2O_3: NiO: K_2O: P_2O_5 ratio 1: 1: 1: 1, pH = 6–7. Final cooling after synthesis to room temperature was done in 24 h. The precipitate was separated by filtering a stock solution, washed several times with hot distilled water and finally dried at room temperature for 12 h. According to optical microscopy study the precipitate is a small green crystal. Crystals were selected manually for further studies.

The element (Bi, Ni and P) contents of the selected crystals were determined by the Jeol JSM6480LV scanning electron microscope equipped with the INCA Wave 500 wave length spectrometer (Laboratory of Local Methods of Matter Investigation, Faculty of Geology, MSU). The conditions of analysis are following: accelerating voltage 20 kV, current 20 nA, beam diameter 3 μm.

2.2. Single-crystal X-ray analysis

A red unshaped grain (0.13 × 0.15 × 0.18 mm^3) was used for single-crystal X-ray data collection. The single-crystal X-ray data were collected at room temperature on a Xcalibur S Oxford Diffraction diffractometer with graphite monochromatized MoK_α radiation (λ = 0.71073 Å) and a CCD detector using the ω scanning mode. Raw data were integrated and then scaled, merged, and corrected for Lorentz-polarization effects using the CrysAlis package [22]. A total of 5873 reflections within the sphere limited by θ = 32.56° were measured. The experimental details of the data collection and refinement results are listed in Table 1. The following unit-cell parameters have been obtained by the least-squares refinement: a = 6.3220 (3) Å, b = 6.9043 (4) Å, c = 7.5641 (5) Å, α = 90.483 (5)°, β = 107.219 (5)°, γ = 110.758 (5)°; V = 292.51 (3) $Å^3$. Space group $P\overline{1}$ (No. 2) was chosen. Atomic scattering factors for neutral atoms together with anomalous dispersion corrections were taken from *International Tables for X-Ray Crystallography* [23]. A structure model was determined by "charge flipping" method using the SUPERFLIP computer program [24]. The structure determination and refinement were carried out using the Jana2006 program package [25]. Illustrations were produced with the JANA2006 program package in combination with the program DIAMOND [26]. The final refinement cycles converged with R_1 = 4.09, wR_2 = 5.23, GoF = 1.00 for 1637 $I > 2\sigma(I)$. The highest peak and deepest minimum in the final residual electron density were 2.39 $eÅ^{-3}$ (near Bi1-site at 0.79 Å) and −2.58 $eÅ^{-3}$ (near Bi2-site 0.81 Å), respectively. The rather big final values of $\Delta\rho_{min}$ and $\Delta\rho_{min}$ indicate the partial disordering of bismuth atoms. However, we could not able to split Bi1-and Bi2-sites, because ADPs of additional sites became non-positive.

Table 2 lists the fractional atomic coordinates, occupancy, site symmetry and equivalent atomic displacement parameters (U_{eq}). Anisotropic atomic displacement parameters (U_{ij}) are presented in Table 3. Selected interatomic distances and angles in the [PO_4] tetrahedra are given in Table 4.

Bond-valence sum calculations (BVS) for $Ni(BiO)_2(PO_4)$ (OH) were calculated using bond valence parameters for Bi^{3+}–O bond [28] and for other bonds (Ni^{2+}–O, and P^{5+}–O) [29]. BVS calculations for the Bi1, Bi2, Ni1, Ni2, and P sites are 2.85, 2.98, 2.00, 2.04, and 4.80 (valence units) (Table 5). In accordance with BVS data for O6 oxygen atom is considerably lower than for other oxygen atoms and corresponds to formation of O6H-group in the $Ni(BiO)_2(PO_4)$ (OH) structure.

Table 1
Crystal data, data collection and refinement of $Ni(BiO)_2(PO_4)(OH)$.

Crystal data	
Formula	$Ni(BiO)_2(PO_4)(OH)$
Formula weight (g)	1239.2
Temperature (K)	293
Cell setting	Triclinic
Space group	$P\overline{1}$ (No. 2)
Lattice Parameters	
a (Å); α (°)	6.3220(3); 90.483(5)
b (Å); β (°)	6.9043(4); 107.219(5)
c (Å); γ (°)	7.5641(5); 110.758(5)
V ($Å^3$)	292.51 (3)
Z	1
Calculated density, Dx ($g\ cm^{-3}$)	7.0349
Crystal size (mm)	0.15 × 0.22 × 0.24
Crystal form	unshaped grain
Crystal color	green
Data Collection	
Diffractometer	Xcalibur Oxford Diffraction (CCD-detector)
Radiation; λ	MoK_α; 0.71073
Absorption coefficient, μ (mm^{-1})	63.456
F (000)	530
Data range θ (°); h, k, l	2.84 −32.56; $-9 < h < 9$, $-10 < k < 10$, $-10 < l < 11$
No. of measured reflections	5873
Total reflections (N_{tot})/unique (N_{ref})	1870/1637
Criterion for observed reflections	$I > 2\sigma(I)$
Refinement	
Refinement on	Full-matrix least squares on F
R_1, wR_2 (all reflection)	4.65/5.23
R, wR ($F > 4\sigma(F)$)	4.09/4.86
R_{int} (%)	7.08
No. of refinement parameters (N_{par})	124
N_{ref}/N_{par}	13.49
Weight scheme	$1/(\sigma^2\|F\| + 0.000841F^2)$
Min./max. residual e density, ($eÅ^{-3}$)	−2.58/2.39*
GoF (Goodness of fit)	1.00

Note: $R_1 = \sum||F_{obs}| - |F_{calc}||/\sum|F_{obs}|$; $wR_2 = \{\sum[w(F^2_{obs} - F^2_{calc})^2]/\sum[w(F^2_{obs})^2]\}^{1/2}$; $GoF = \{\sum[w(F^2_{obs} - F^2_{calc})]/(n-p)\}^{1/2}$ where n is a number of reflections and p is a number of refined parameters.

Table 2
Fractional atomic coordinates, site symmetry, and equivalent atomic displacement parameters (U_{eq}) for $Ni(BiO)_2(PO_4)(OH)$.

Atom	x	y	z	Site	U_{eq}
Bi1	0.0025(2)	0.2844(2)	0.1229(1)	2*i*	0.0096(2)
Bi2	0.0305(2)	0.7290(1)	0.3831(1)	2*i*	0.0097(2)
Ni1	0.5	0.5	0.5	1*h*	0.0077(6)
Ni2	−0.5	0.5	0	1*e*	0.0076(6)
P	−0.430(1)	−0.103(1)	0.272(1)	2*i*	0.0089(8)
O1	−0.704(3)	−0.154(1)	0.206(1)	2*i*	0.012(2)
O2	−0.148(1)	0.525(1)	0.086(1)	2*i*	0.008(2)
O3	0.849(1)	0.524(1)	0.586(1)	2*i*	0.006(2)
O4	−0.358(1)	−0.188(1)	0.120(1)	2*i*	0.015(3)
O5	−0.294(1)	0.138(1)	0.308(1)	2*i*	0.009(2)
OH6	−0.427(1)	0.611(1)	−0.230(1)	2*i*	0.010(2)
O7	−0.352(1)	−0.187(1)	0.459(1)	2*i*	0.017(3)

Note: U_{eq} is defined as one third of the trace of the orthogonalized U_{ij} tensor.

2.3. Vibrational spectroscopy

The infrared spectrum of $Ni(BiO)_2PO_4(OH)$ was obtained on an FSM 12011 FTIR spectrometer at the region from 4000 to 400 cm^{-1} at

Table 3
Anisotropic atomic displacement parameters for $Ni(BiO)_2(PO_4)(OH)$.

Site	U^{11}	U^{22}	U^{33}	U^{12}	U^{13}	U^{23}
Bi1	0.0109(2)	0.0068(2)	0.0089(2)	0.0021(1)	0.0014(1)	0.0001(1)
Bi2	0.0108(2)	0.0078(2)	0.0088 (2)	0.0030 (1)	0.0011 (1)	−0.0000 (1)
Ni1	0.0055 (7)	0.0077 (8)	0.0060 (8)	0.0003 (6)	−0.0008(6)	−0.0010(6)
Ni2	0.0064(7)	0.0073(8)	0.0068(8)	0.0015(6)	0.0001(6)	−0.0009(6)
P	0.011(1)	0.005(1)	0.008(1)	0.0013(8)	0.0019(9)	−0.0024(8)
O1	0.007(3)	0.014(4)	0.012(3)	−0.001(3)	0.004(3)	−0.003(3)
O2	0.008(3)	0.003(3)	0.012(3)	0.000(2)	0.003(3)	0.003(3)
O3	0.003(3)	0.005(3)	0.005(3)	−0.003(2)	0.001(2)	−0.002(2)
O4	0.020(4)	0.015(4)	0.008 (3)	0.001 (3)	0.010 (3)	0.001 (3)
O5	0.014 (3)	0.005 (3)	0.007 (3)	0.001 (3)	0.002(3)	0.001(2)
O6	0.011(3)	0.014(3)	0.002(3)	0.003(3)	0.000(2)	−0.003(3)
O7	0.017(4)	0.019(4)	0.012(4)	0.006(3)	0.003(3)	0.001(3)

Table 4
Selected interatomic distances (Å) and angles in the $[PO_4]$ tetrahedra for $Ni(BiO)_2(PO_4)(OH)$.

Bond		d, Å	Bond		d, Å
Bi1	−O2	2.172(9)	Ni2	OH6	2.015(7) × 2
	−O2	2.262(8)		O2	2.067(8) × 2
	−O3	2.310(7)		O4	2.092(8) × 2
	−OH6	2.391(7)	⟨Ni2−O⟩		2.058
	−O1	2.559(7)	Δ^{Ni2}		2.429
	−O5	2.594(9)	P	−O4	1.533(11)
	−O4	3.248(2)		−O7	1.545(9)
⟨Bi1−O⟩		2.505		−O1	1.558(8)
Bi2	−O3	2.128(9)		−O5	1.559(7)
	−O3	2.364(8)	⟨P−O⟩		1.549
	−O2	2.371(7)	Angle, °		
	−O5	2.376(6)	O1−P−O4		110.7(5)
	−O1	2.377(9)	O1−P−O5		109.3(5)
	−O7	2.887(10)	O1−P−O7		110.5(5)
	−O4	2.904(8)	O4−P−O5		107.6(4)
	−O7	3.083(8)	O4−P−O7		112.0(5)
⟨Bi1−O⟩		2.561	O5−P−O7		106.6(4)
Ni1	OH6	2.037(7) × 2			
	O3	2.054(7) × 2			
	O7	2.094(8) × 2			
⟨Ni1−O⟩		2.062			
Δ^{Ni1}		1.343			

Note: Octahedral distortion was calculated using follow equation [27]: $\Delta = (1/6)\sum_{i=1-6}\{[(M-O)_i - \langle M-O\rangle]/\langle M-O\rangle\}^2 \times 10^4$.

Table 5
Bond valence calculation for $Ni(BiO)_2(PO_4)(OH)$.

Atom	Bi1	Bi2	Ni1	Ni2	P	$\sum_v a$
O1	0.31	0.45			1.17	1.93
O2	0.68 + 0.57	0.46		$0.33_{\times 2\downarrow}$		2.04
O3	0.51	0.75 + 0.46	$0.34_{\times 2\downarrow}$			2.06
O4	0.07	0.15		$0.31_{\times 2\downarrow}$	1.25	1.78
O5	0.28	0.46			1.17	1.91
OH6	0.43		$0.36_{\times 2\downarrow}$	$0.38_{\times 2\downarrow}$		1.17
O7		0.15 + 0.10	$0.30_{\times 2\downarrow}$		1.21	1.76
$\sum_v c$	2.85	2.98	2.00	2.04	4.80	

$\sum_v \boldsymbol{a}$ and $\sum_v \boldsymbol{c}$ are the bond valence sums for anions and cations, respectively.
The × 2↓ sign indicates the doubling of the corresponding valence contributions in columns due to symmetry.

ambient conditions. The spectral resolution was approximately 2 cm^{-1}. The transmission spectra in the mid-IR were studied by forming a tablet with the sample mixed with dry KBr powder.

The Raman spectrum of Bi-Ni phosphate $Ni(BiO)_2(PO_4)(OH)$ was obtained using an EnSpectr R532-50 instrument with a green laser (λ = 532 nm) at room temperature. The power of the laser beam at the sample was ~15 mW. The spectrum was recorded from 100 to 4000 cm^{-1} with resolution ~6 cm^{-1}. The diameter of the focal spot on the sample was ~15 μm. Signal acquisition time for a single scan of the spectral range was 3000 ms and the signal was averaged over 30 scans. The Raman spectrum was obtained from a randomly oriented crystal.

3. Results

3.1. Crystal structure

The crystal structure of a new $Ni(BiO)_2PO_4(OH)$ compound (Fig. 1) is similar to the structure of namibite $Cu(BiO)_2VO_4(OH)$ [30] and based on infinite chains $\{M\emptyset(TO_4)\}_\infty^{n-}$ ($M = Ni^{2+}$, Cu^{2+}; $T = P^{5+}$, V^{5+}, and $\emptyset = OH^-$) going along *c*. Each chain is formed by the octahedral rod of $[MO_4\emptyset_2]$-octahedra linking *via* common *trans* Ø-vertexes (Fig. 2a). The environment around symmetrically non-equivalent $M1\varphi_6$-and $M2\varphi_6$-octahedra is more regular ($\Delta^{Ni1} = 1.343$; $\Delta^{Ni2} = 2.429$) in the structure of a new compound [where $M = Ni^{2+}$ ($3d^8$)] whereas in the structure of namibite these polyhedra are characterized by the Jahn-Teller distortion, as expected from $M = Cu^{2+}$, a $3d^9$ ion. Rods are decorated with $[TO_4]$-tetrahedra in a staggered arrangement. Adjacent chains are linked along *b* period predominantly *via* hydrogen bonds of hydroxyl groups (Fig. 2b). Because of the absence of hydrogen position obtained from single-crystal X-ray analysis the geometry of H-bond is questionable, but we are able to expect the bond between O6 (donor) oxygen atom of OH group and O5 (acceptor) oxygen atom which is apical vertex of $[PO_4]$-tetrahedra with distance $D-A = 2.835$ Å (Fig. 2c).

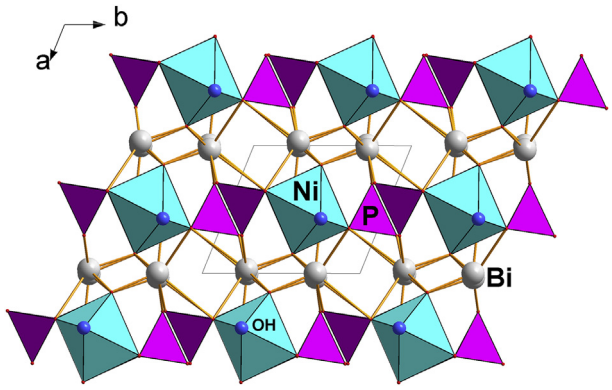

Fig. 1. General view of $Ni(BiO)_2(PO_4)(OH)$ structure projected on (001).

Heteropolyhedral chains alternates with layers of Bi atoms which are also parallel to (100) (Fig. 3a). Bismuth atoms form distorted Bi1φ_7-and Bi2φ_8-polyhedra (consequently strong bonds in one coordination hemisphere and longer weak bonds in another; Fig. 3b and c, respectively) which can be explained by stereoactivity of lone electron pair on the Bi^{3+} cations.

The structure of $Ni(BiO)_2PO_4(OH)$ as well as namibite are characterized by the presence of 'additional' oxygen atoms and OH-group and could be described in the terms of anion-centered crystal chemistry [5]. Atoms O2 and O3 are tetrahedrally coordinated by three Bi^{3+} and one Ni^{2+} cations with mean distances O2-*Me* = 2.218 Å and O3-*Me* = 2.214 Å. [$ONiBi_3$]-tetrahedra linking *via* common edges form double *einer* chain of ***C*3**-type [31] going along *c*. Oxygen O6 atom belonging to hydroxyl group form [ONi_2Bi]-triangle ($\langle O2-Me\rangle$ = 2.147 Å) and attached additionally to the tetrahedral chain. Condensation of the chains leads to formation of heteropolyhedral $[O_2(OH)NiBi_2]^{3+}$-layer which is parallel (010) (Fig. 4a). The interlayer space is occupied by isolated $[PO_4]^{3-}$-tetrahedron (Fig. 4b).

3.2. Vibrational spectroscopy

IR and Raman spectra of new Bi–Ni phosphate are shown in Fig. 5. The bands in the region 1055–450 cm^{-1} in vibrational spectra are typical for orthophosphates [32]. The crystal structure contains one position of phosphorus atoms with C_1 symmetry (2*i*). That leads to following vibrations of PO_4^{3-} tetrahedral units: $\nu_3 - 3A_u + 3A_g$, ν_1-$A_u + A_g$, $\nu_4 - 3A_u + 3A_g$ and $\nu_2 - 2A_u + 2A_g$. A_u modes are active in IR spectra and A_g modes are active in Raman spectra. The bands at 1052, 1007 and 937 cm^{-1} in IR spectra and at 997 and 955 cm^{-1} in Raman spectra are assigned to the asymmetric valence ν_3 oscillations. The band at 929 cm^{-1} in both vibrational spectra belongs to symmetric valence ν_1 vibrations of PO_4^{3-} units. The group of bands in the region 600–530 cm^{-1} is ascribed to asymmetrical bending ν_4 vibrations of PO_4^{3-} units. This group in IR spectrum contains more bands than predicted by theoretical analysis, it may contain additional band due to in-plane Ni–O–H bending vibrations [33]. The bands at 490–450 cm^{-1} attribute to ν_2 symmetrical bending vibrations of PO_4^{3-} tetrahedra. The weak band at 811 cm^{-1} in IR spectrum does not fit into the pattern of the infrared absorption spectra of phosphates and, probably, may be assigned to the hydroxyl-bending modes of the OH unit. The similar bands have been described in pseudomalachite, libethenite, and cornetite [34] and amblygonite-montebrasite IR spectra [35]. The bands in the low-frequency region (<420 cm^{-1}) are related to external modes.

The OH stretching vibrations region of IR spectrum of $Ni(BiO)_2(PO_4)(OH)$ is shown in the Fig. 6. In this region one strong band at 3327 cm^{-1} with two weak shoulders (3372, 3261 cm^{-1}) is observed. As the bonds O6–O2, O6–O3, O6–O4 and O6–O7 represent edges of the NiO_6 octahedra, so we expect O5 as the acceptor atom of an H bond. OH stretching frequency (3327 cm^{-1}) corresponds well to *d* (O6H···O5) distance 2.835 Å [36]. However, two oxygen atoms (O4 and O7) have low incident bond-valence sums (1.78 and 1.76 v. u. respectively), so we can suggest the possibility of somewhat disordering of H position so that O4 and O7 oxygen atoms might participate in weak H bonding (Fig. 7).

4. Magnetic properties

Since the crystal structure of $Ni(BiO)_2PO_4(OH)$ (**1**) and parent mineral namibite $Cu(BiO)_2VO_4(OH)$ (**2**) contains distinct isolated chains composed of oxo-bridged magnetic 3 d-ions (Fig. 4), these compounds can potentially exhibit some low-dimensional (1D) magnetic behavior at low temperature (see e.g. Ref. [37]). It is therefore of interest to evaluate magnetic properties of **1** and **2**. For this, we estimate exchange parameters *J* describing isotropic spin coupling $-JS_iS_j$ of magnetic 3 d ions within chain (J_1) and between chain (J_2). Exchange parameters are obtained from microscopic

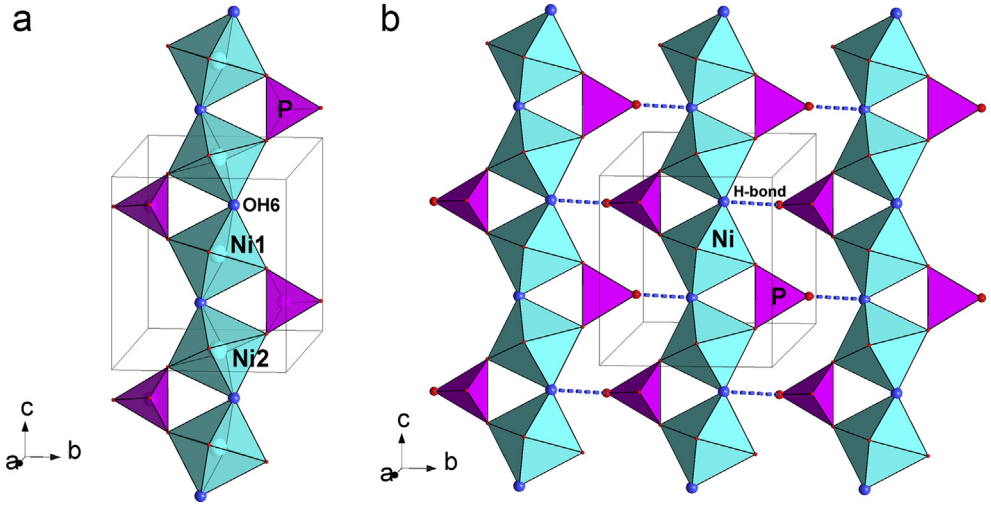

Fig. 2. Infinite chains $\{M\emptyset(TO_4)\}_\infty^{n-}$ (a) and heteropolyhedral pseudolayer (b) in the structure of $Ni(BiO)_2(PO_4)(OH)$.

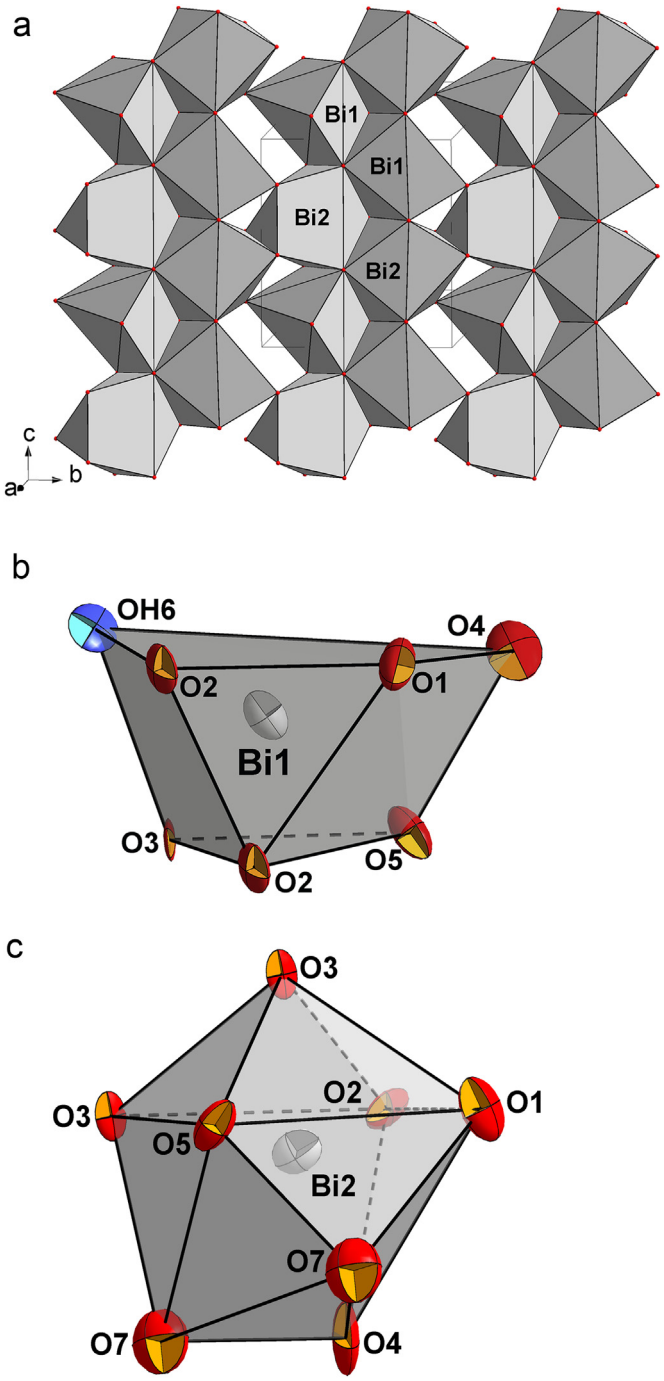

Fig. 3. Bismuth layer in the structure of $Ni(BiO)_2(PO_4)(OH)$ (a) and coordination environment of Bi1- (b) and Bi2-sites (c).

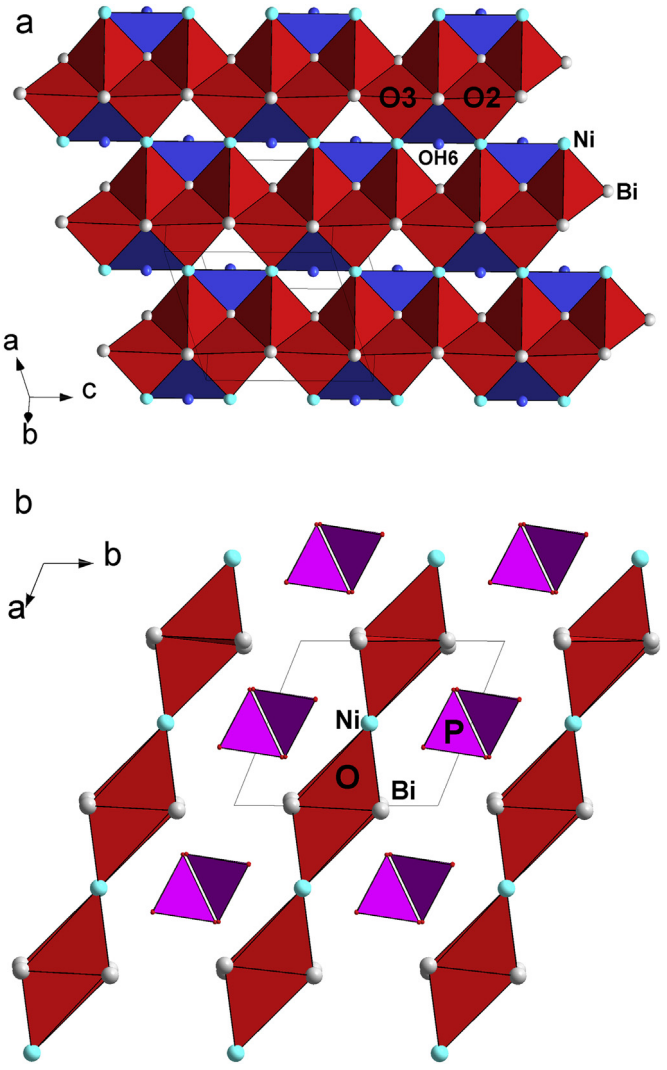

Fig. 4. Heteropolyhedral $[O_2(OH)NiBi_2]^{3+}$-layer (a) and general view [projected on (001)] of the $Ni(BiO)_2(PO_4)(OH)$ structure (b) shown in the terms of anion-centered crystal chemistry.

calculations in terms of a many-electron superexchange model following computational approach described in Refs. [38–40]. In these calculations, the electronic structure and magnetic properties of individual Ni^{2+} and Cu^{2+} ions in compounds **1** and **2** are analyzed in terms of ligand-field (LF) calculations combined with the angular-overlap model (AOM) [41]; this provides a more realistic description of the ground-state wave functions of Ni^{2+} and Cu^{2+} ions in the actual low-symmetry coordination of magnetic sites in **1** and **2**. For Ni^{2+} ions, we use $B = 850$ and $C = 3800$ cm^{-1} Racah parameters (which are typical average value of B and C parameters for Ni^{2+} ions in oxide host matrices [42]) and $\zeta = 600$ cm^{-1} spin-orbit coupling constant. Typical AOM parameters are employed for divalent 3 d ions, $e_\sigma = 4000$ and $e_\pi = 1000$ cm^{-1} (at the average metal-ligand distance R_0); the radial dependence of these parameters is approximated by $e_{\sigma,\pi}(R) = e_{\sigma,\pi}(R_0)\,(R_0/R)^n$ with $n = 4$. These LF calculations indicate that Ni^{2+} ions in **1** have a well-isolated triplet ground spin state $^3A_2$ ($S = 1$) with two unpaired electrons on x^2-y^2 and z^2 orbitals; in compound **2**, Cu^{2+} ions have one unpaired electron occupying magnetic orbital of the x^2-y^2 type.

In order to evaluate intrachain exchange parameter J_1, we selected isolated exchange-coupled pairs of magnetic ions taken from the actual crystal structure of **1** and **2**, Fig. 8. The electron transfer parameters (one-electron matrix elements connecting magnetic 3 d orbitals on two exchange-coupled Ni or Cu centers) are obtained from extended Huckel calculations (using standard atomic parameterization [http://www.op.titech.ac.jp/lab/mori/EHTB/EHTB.htm]). Electron transfer parameters are derived by projection of 3 d-rich molecular orbitals of the Ni–Ni pair onto pure 3 d atomic orbitals of two metal atoms, as described in Ref. [43] (see also [38–40] for more detail). The Ni↔Ni and Cu↔Cu charge-transfer energy is set to 65,000 cm^{-1} (8 eV); this approach has been previously used to analyze magnetic properties of a polymeric

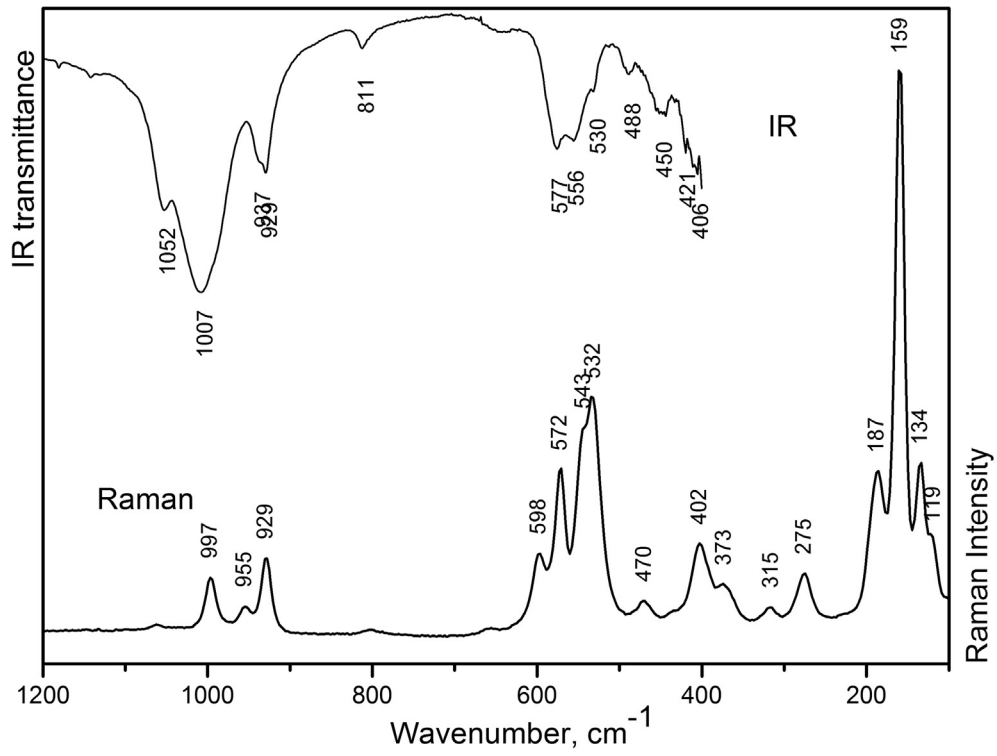

Fig. 5. Vibrational (infrared and raman) spectra of $Ni(BiO)_2(PO_4)(OH)$.

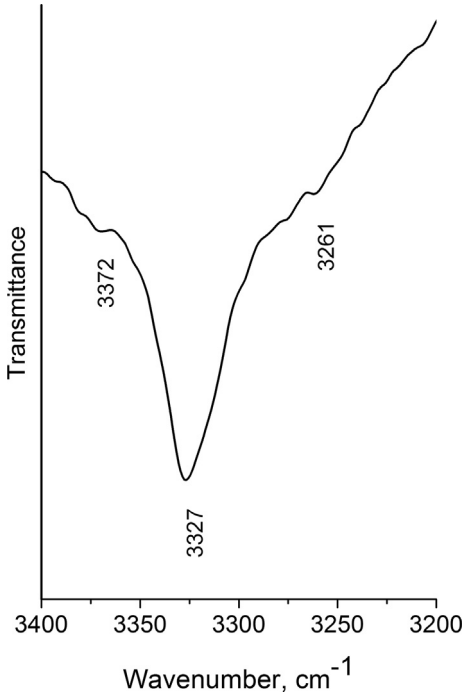

Fig. 6. IR spectrum of $Ni(BiO)_2(PO_4)(OH)$ in the region of OH stretching vibrations.

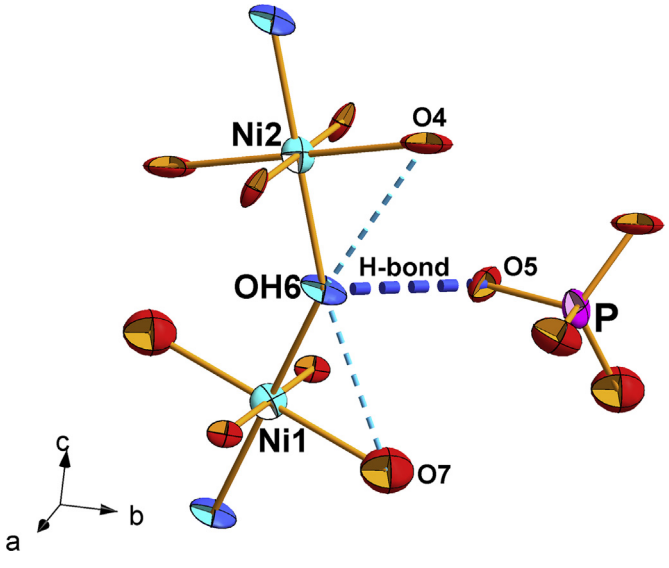

Fig. 7. The system of hydrogen bonds in the structure of $Ni(BiO)_2(PO_4)(OH)$.

Ni(II) compound [39]. Our calculations show that the intrachain spin coupling between Ni^{2+} ions in **1** is weakly antiferromagnetic, $J_1(Ni{-}Ni) = -2.1$ cm^{-1}. On the other hand, similar calculations for extended exchange-coupled clusters (involving actual Ni–Ni exchange-coupled pairs connecting neighboring magnetic chains, see Fig. 4b) indicate very weak interchain spin coupling, $J_2 \sim -0.15$ cm^{-1}. Therefore, at low temperature (T < 20 K) $Ni(BiO)_2PO_4(OH)$ may potentially display an interesting magnetic behavior typical of one-dimensional $S = 1$ spin systems (see e.g. Ref. [44]). Interestingly, our LF calculations indicate that the zero-field splitting energy (ZFS) of Ni^{2+} ions in **1** is rather large and positive ($D_{ZFS} = -5.8$ cm^{-1}, $E_{ZFS} \sim 0$); in fact, it is comparable to the spin-coupling energy $-J_1\boldsymbol{S}_i\boldsymbol{S}_j$. This suggests possible complicated magnetic behavior of $Ni(BiO)_2PO_4(OH)$ at low temperature.

By contrast, our calculations for the parent namibite compound $Cu(BiO)_2VO_4(OH)$ resulted in a ferromagnetic intrachain spin coupling between Cu^{2+} ions, $J_1 = +9.3$ cm^{-1}. The origin of

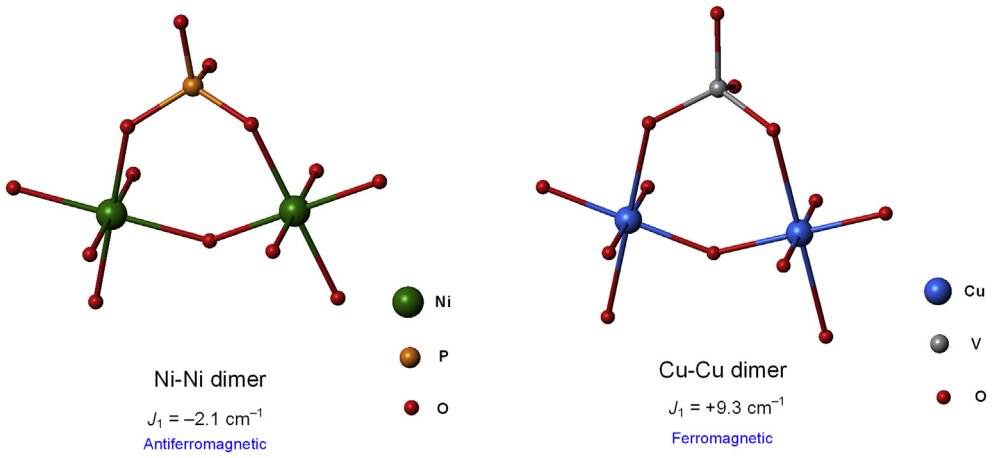

Fig. 8. The local structure of Ni–Ni and Cu–Cu exchange-coupled pairs in $Ni(BiO)_2PO_4(OH)$ and $Cu(BiO)_2VO_4(OH)$ and calculated exchange parameters.

ferromagnetism is seemingly related to a bent structure of the Cu–O–Cu bridging group combined with electron transfer processes mediated by the diamagnetic VO_4 group. More quantitatively, in this case ferromagnetism is due to a large electron-transfer matrix element connecting half-filled $x^2–y^2$ orbital on one Cu^{2+} center and doubly-occupied xy orbital on the second Cu^{2+} center in the exchange coupled pair. Again, calculations indicate very small interchain spin coupling, J_2(Cu–Cu) ~ −0.05 cm^{-1}. Therefore at low temperature $Cu(BiO)_2VO_4(OH)$ may exhibit ferromagnetic properties typical of quasi-one-dimensional S = 1/2 quantum ferromagnets [45].

5. Conclusion

In summary, new $Ni(BiO)_2PO_4(OH)$ compound is prepared by hydrothermal synthesis and characterized by single-crystal X-ray analysis, Raman- and IR-spectroscopy. It is the second representative of the family of compounds with a namibite-type structure, in which high-spin Ni^{2+} ions form isolated 1D magnetic chains. Our microscopic calculations of the intra- and interchain J (Ni–Ni) exchange parameters indicate that at low temperatures this compound may exhibit $S = 1$ antiferromagnet chain behaviour. We hope that our results will stimulate further efforts to synthesis and study of new materials with general formula $M(BiO)_2(XO_4)(OH)$ (where M is transitional metal and X = P, V) because of their potentially interesting structural and magnetic properties.

Acknowledgements

S.M.A and D.V.D. are grateful for financial support of the Foundation of the President of the Russian Federation (Grant Nos: MK-8990.2016.5 and MK-7926.2016.5).

References

[1] C.W.M. Timmermans, G.J. Blasse, J. Solid State Chem. 52 (1984) 222.
[2] S. Wu, C. Wang, Y. Cui, T. Wand, B. Huang, X. Zhang, X. Qin, P. Brault, Mat. Lett. 64 (2010) 115.
[3] R. Burch, S. Chalker, P. Loader, J.M. Thomas, W. Ueda, J. Appl. Catal. A 82 (1992) 77.
[4] S. Liu, W. Miiller, Y. Liu, M. Avdeev, C.D. Ling, Chem. Mater. 24 (2012) 3932.
[5] S.V. Krivovichev, O. Mentré, O. Siidra, M. Colmont, S.K. Filatov, Chem. Rev. 113 (2013) 6459.
[6] D. Endara, M. Colmont, M. Huvé, G. Tricot, L. Carpentier, O. Mentré, Inorg. Chem. 51 (2012) 4438.
[7] M. Huvé, M. Colmont, J. Lejay, P. Aschehoug, O. Mentré, Chem. Mater. 21 (2009) 4019.
[8] D. Endara, M. Colmont, M. Huvé, F. Capet, J. Lejay, J. Aschehoug, O. Mentré, Inorg. Chem. 51 (2012) 9557.
[9] M. Huvé, M. Colmont, O. Mentré, Chem. Mater 16 (2004) 2628.
[10] M. Colmont, M. Huvé, O. Mentré, Inorg. Chem. 45 (2006) 6612.
[11] M. Huvé, M. Colmont, O. Mentré, Inorg. Chem. 45 (2006) 6604.
[12] A. Aliev, D. Endara, M. Huvé, M. Colmont, P. Roussel, L. Delevoye, T.T. Tran, P.S. Halasyamani, O. Mentré, Inorg. Chem. 53 (2014) 861.
[13] M. Lü, M. Colmont, H. Kabbour, S. Colis, O. Mentré, Inorg. Chem. 53 (2014) 6969.
[14] M.S. Kozin, A. Aliev, M. Colmont, O. Mentré, O.I. Siidra, S.V. Krivovichev, J. Solid State Chem. 199 (2013) 56.
[15] M.S. Kozin, M. Colmont, D. Endara, A. Aliev, M. Huvé, O.I. Siidra, S.V. Krivovichev, O. Mentré, J. Solid State Chem. 199 (2013) 123.
[16] M. Colmont, D. Endara, A. Aliev, C. Terryn, M. Huvé, O. Mentré, J. Solid State Chem. 203 (2013) 266.
[17] A. Aliev, M.S. Kozin, M. Colmont, O.I. Siidra, S.V. Krivovichev, O. Mentré, Phys. Chem. Miner. 42 (2015) 663.
[18] F. Abraham, M. Ketatni, G. Mairesse, B. Mernari, Eur. J. Solid State Inorg. Chem. 31 (1994) 313.
[19] N. Arumugam, V. Lynch, H. Steinfink, J. Solid State Chem. 181 (2008) 2313.
[20] W.-L. Zhang, Z.-Z. He, T.-L. Xia, Z.-Z. Luo, H. Zhang, C.-S. Lin, W.-D. Cheng, Inorg. Chem. 51 (2012) 8842.
[21] A.C. Roberts, P.C. Burns, R.A. Gault, A.J. Criddle, M.N. Feinglos, J.A.R. Stirling, Eur. J. Mineral. 13 (2001) 167.
[22] Oxford Diffraction, CrysAlisPro, Oxford Diffraction Ltd, Abingdon, Oxfordshire, UK, 2009.
[23] J.A. Ibers, W.C. Hamilton (Eds.), International Tables for X-ray Crystallography IV, The Kynoch Press, Birmingham, UK, 1974.
[24] L. Palatinus, G. Chapuis, J. Appl. Cryst. 40 (2007) 786.
[25] V. Petříček, M. Dušek, L. Palatinus, Jana, Structure Determination Software Programs, 2006, Institute of Physics, Praha, Czech Republic, 2006.
[26] K. Brandenburg, DIAMOND, Version 2.1c, Crystal Impact GbR, Bonn, Germany, 1999.
[27] I.D. Brown, R.D. Shannon, Acta Crystallogr. A 29 (1973) 266.
[28] S. V. Krivovichev, Z. Kristallogr. 227 (2012) 575.
[29] I.D. Brown, D. Altermatt, Acta Crystallogr. B 41 (1985) 244.
[30] U. Kolitsch, U. Giester, Am. Mineralogist 85 (2000) 1298.
[31] S.V. Krivovichev, S.K. Filatov, Crystal Chemistry of Minerals and Inorganic Compounds with Complexes of Anion-centered Tetrahedra, St. Petersburg University Press, St. Petersburg (, 2001.
[32] V.S. Farmer (Ed.), Infrared Spectra of Minerals. Mineral Society, Adlard and Son Ltd, London, 1974, p. 278.
[33] D.N. Yang, R.M. Wang, M.S. He, J. Zhang, Z.F. Liu, J. Phys. Chem. B 109 (2005) 7654.
[34] W. Martens, R.L. Frost, Am. Mineralogist 88 (2003) 37.
[35] A.M. Fransolet, P. Tarte, Am. Mineralogist 62 (1977) 559.
[36] E. Libowitzky, Mh Chemie 130 (1999) 1047.
[37] M. Takahashi, Progress in Theoret. Phys. Suppl. vol. 87 (1986) 233.
[38] V.S. Mironov, L.F. Chibotaru, A. Ceulemans, Phys. Rev. B 67 (2003) 014424.
[39] M.E. Nikiforova, M.A. Kiskin, A.S. Bogomyakov, G.G. Aleksandrov, A.A. Sidorov, V.S. Mironov, I.L. Eremenko, Inorg. Chem. Commun. 14 (2011) 362.
[40] E.N. Zorina, N.V. Zauzolkova, A.A. Sidorov, G.G. Aleksandrov, A.S. Lermontov, M.A. Kiskin, A.S. Bogomyakov, V.S. Mironov, V.M. Novotortsev, I.L. Eremenko, Inorg. Chim. Acta 396 (2013) 108.
[41] C.E. Schaffer, Struct. Bond. 5 (1968) 68.
[42] M.G. Brik, A.M. Srivastava, N.M. Avram, A. Suchocki, J. Luminescence 148 (2014) 338.
[43] S.J. Lee, J. Am. Chem. Soc. 111 (1989) 7754.
[44] M.D. Lumsden, G.E. Granroth, D. Mandrus, S.E. Nagler, J.R. Thompson, J.P. Castellan, B.D. Gaulin, Phys. Rev. B 62 (2000) R9245.
[45] C.P. Landee, R.D. Willett, Phys. Rev. Lett. 43 (1979) 463.